Hypoxia inducible factor-1α is necessary for invasive phenotype in *Vegf*-deleted islet cell tumors

Authors

Takaaki Takeda[1, 3], Hiroaki Okuyama[2], Yasuko Nishizawa[2, 3], Shuhei Tomita[4], Masahiro Inoue[1,3]

Affiliations

[1]Department of Biochemistry and [2]Pathology, Osaka Medical Center for Cancer and Cardiovascular Diseases, Higashinari-ku, Osaka 537-8511, Japan. [3]Department of Clinical and Experimental Pathophysiology, Osaka University, Graduate School of Pharmaceutical Sciences, Suita, Osaka 565-0871, Japan. [4]Department of Pharmacology, Institute of Health Biosciences, The University of Tokushima, Tokushima 770-8503, Japan

Address correspondence to：

Masahiro Inoue

Department of Biochemistry, Osaka Medical Center for Cancer and Cardiovascular Diseases, Higashinari-ku, Osaka 537-8511, Japan

Tel: +81-6-6972-1181, Fax: +81-6-6973-5691

E-mail: inoue-ma2@mc.pref.osaka.jp

## Supplementary figure S1

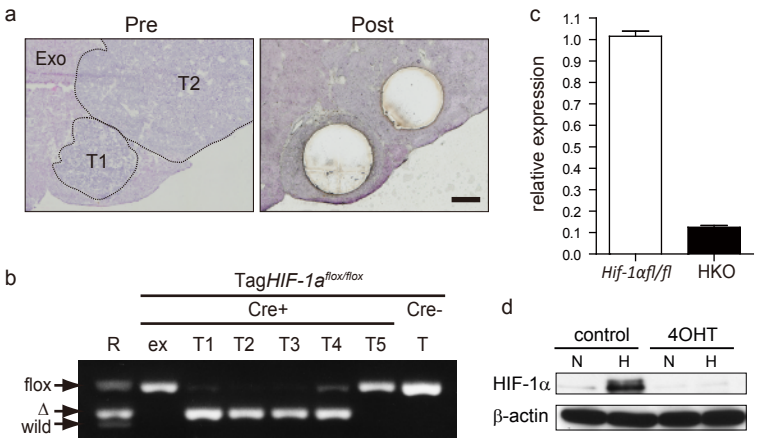


## Supplementary figure S2

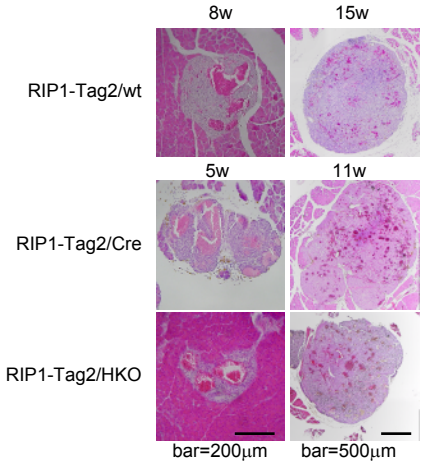

Supplementary figure S3

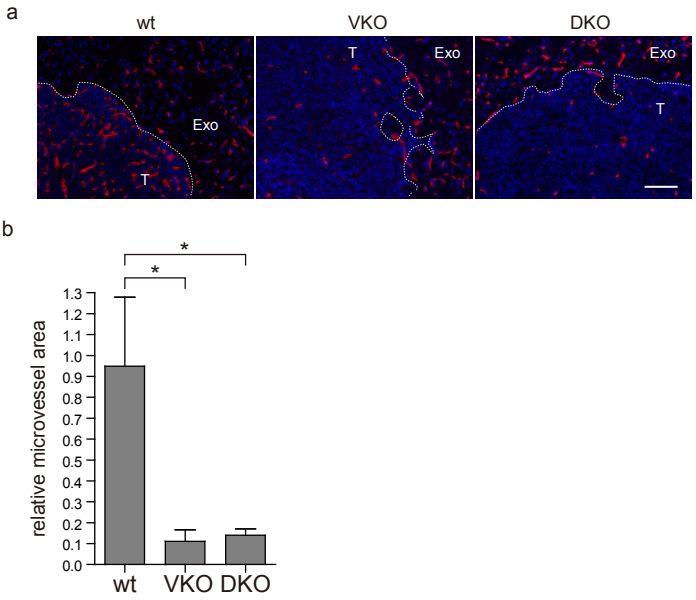


Supplementary figure S4

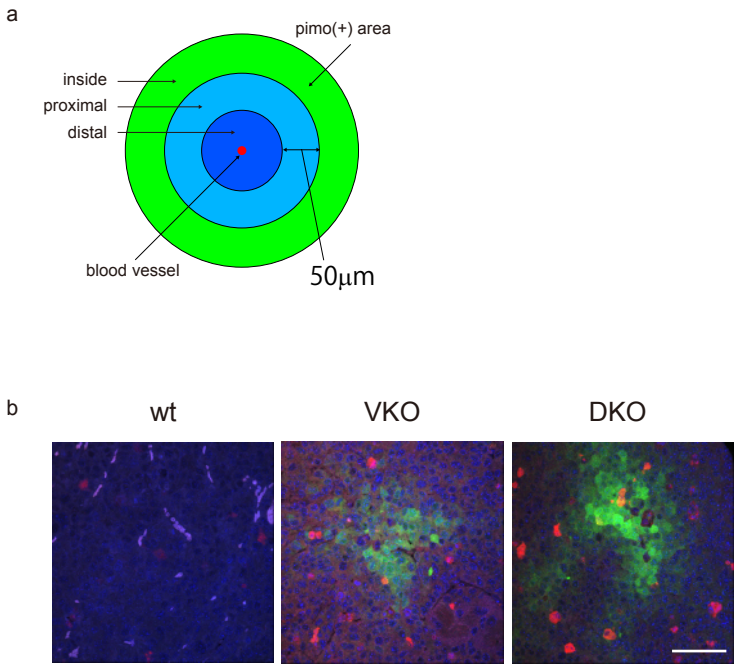

Supplementary figure S5

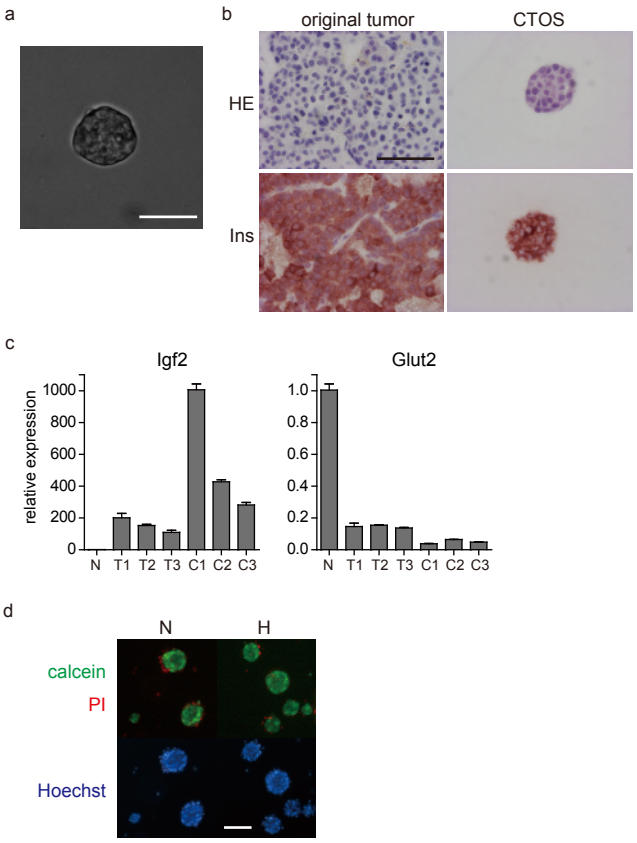


Supplementary figure S6

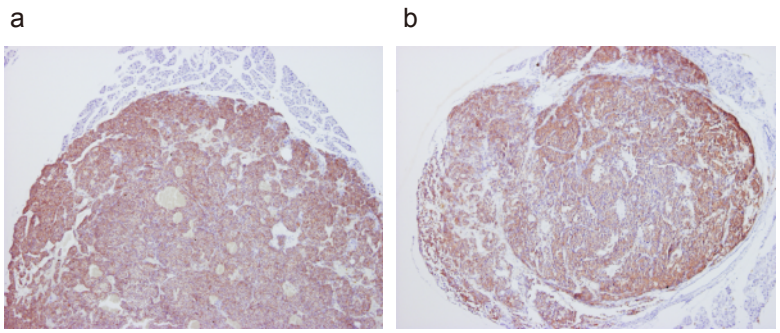


Wt tumor at 15w

HKO tumor at 11w

## Supplementary Figure Legends

**Supplementary Figure S1 | Tissue-specific deletion of *HIF-1α* in the islets of pancreas.** To confirm whether *Hif-1α* was deleted in the tumors of RIP1-Tag2/HKO mice, the tumors were micro-dissected. DNA was extracted from each tumor and then PCR analysis was performed to detect floxed and deleted alleles of *Hif-1α*. Adjacent exocrine tissue was used as an internal control. Mice not carrying the *RipCre* gene (RIP1-Tag2*/Hif-1α*$^{fl/fl}$) were used as controls. The recombined allele was detected in the tumors but not in the exocrine tissue of RIP1-Tag2/HKO mice, nor in the tumors of RIP1-Tag2*/Hif-1α*$^{fl/fl}$. One out of nine tumors did not show recombination, even in RIP1-Tag2/HKO, which is approximately the same efficacy of Cre/lox system as previously reported [1]. Next, we examined the efficacy of *Hif-1α* deletion at the mRNA level. RNA was extracted from RipTag tumors of *RipCre/Hif-1α*$^{fl/fl}$ and *Hif-1α*$^{fl/fl}$ mice, and reverse transcribed to cDNA. A remarkable decrease of Hif-1*α* mRNA levels was observed in RIP1-Tag2/HKO tumors compared with RIP1-Tag2*/Hif-1α*$^{fl/fl}$ tumors. To assess the efficacy of *Hif-1α* deletion at the protein level, we examined cell lines established from islet tumors of RIP1-Tag2/HKO mice. A retrovirus vector of inducible Cre was permanently transfected, creating RipTag/CreERT/*Hif-1α*$^{fl/fl}$ cells. Hif-1α protein, which was induced by hypoxia, was diminished after tamoxifen treatment in RipTag/CreERT/*Hif-1α*$^{fl/fl}$ cells. Taken together, deletion of *Hif-1α* was confirmed at the levels of DNA, mRNA, and protein.

(**a**) Genotyping of *Hif-1α* in RipTag tumors. H&E staining of the tumors from a RipTag/HKO mouse. Pre, before micro-dissection; Post, after micro-dissection. T1 and T2, tumors; Exo, exocrine tissue. Scale bar, 200 μm. (**b**) PCR analysis of *Hif-1α*. Genome DNA was extracted from micro-dissected tissues of the exocrine pancreas (Exo), and the tumors (T). A RipTag/*Hif-1α*$^{fl/fl}$ mouse and a RipTag/RipCre/*Hif-1α*$^{fl/fl}$ mouse were examined. Reference (R) bands at the left end lane are the PCR products from the tail DNA of a *Hif-1α*$^{fl/wt}$ mouse (flox and wild), and the tumors of a RipTag/RipCre/*Hif-1α*$^{fl/fl}$ mouse (Δ). The expected sizes of the PCR products are floxed allele (flox): 441 bp, recombined allele (Δ): 355 bp, and wild-type allele (wild), 325 bp. (**c**) Expression levels of

Hif-1α in RipTag tumors. Tumors were isolated from RipTag/*Hif-1α*$^{fl/fl}$ (wt) and RipTag/RipCre/*Hif-1α*$^{fl/fl}$ (HKO) mice; mRNA was extracted and subjected to real-time RT-PCR for Hif-1α. Relative expression to the RipTag/wt tumor is shown. (**d**) Western blotting of Hif-1α in the cell line generated from a RipTag/*Hif-1α*$^{fl/fl}$ mouse. The cell lines transfected with the CreERT gene were treated with either ethanol as a control or 100 nM 4OHT for 24 h. Then, the cells were cultured under normoxic (N) or hypoxic (H) conditions for 24 h, and subjected to western blotting. ß-actin is shown as a loading control.

**Supplementary Figure S2 | Morphology of the tumors in RIP1-Tag2/wt, Cre, and HKO mice.** Angiogenic islets (left panels) and islet tumors (right panels) are shown. Mouse genotypes and ages are indicated.

**Supplementary Figure S3 | Microvessel area in the tumors.** (**a**) Immunohistochemical staining of CD31. T, tumor; Exo, exocrine tissue. The boundary of the tumor and the exocrine pancreas are traced with a dotted line. Scale bar, 100 μm. (**b**) Quantification of microvessel area. Relative values to the adjacent exocrine tissue are shown. Wt mice ($n$ = 4, 5 tumors); RipTag/VKO ($n$ = 4, 5 tumors); RipTag/DKO ($n$ = 3, 5 tumors). The values were standardized by that of the adjacent exocrine tissue and are shown as mean ± SD. *$P$ < 0.05.

**Supplementary Figure S4a | Schematic diagram indicating the regions with different staining pattern of pimonidazole.** Inside, the pimonidazole staining area; proximal, the area adjacent to the pimonidazole staining area (within 50 μm); distal, area more than 50 μm from the pimonidazole staining area.

**Supplementary Figure S4b | Mode of death in the tumors.**Immunohistochemical staining of caspase-3. Red: caspase-3, green: pimonidazole, blue:DAPI. Scale bar: 50μm

**Supplementary Figure S5 | Characteristics of COTSs from RipTag tumors.** (**a**) Phase contrast image of a CTOS from a RipTag/wt tumor. Scale bar, 50μm. (**b**) H&E staining

(upper panels), and insulin (Ins) staining (lower panels) of original tumors (left panels) and CTOSs (right panels). Scale bar, 50μm. (**c**) Real-time RT-PCR analysis of CTOSs. Expressions of Igf2 and Glut2 mRNA were analyzed. Normal islets from C57Bl/6 mice (N), three tumors (T1-3), and CTOSs from three tumors were prepared from a wild-type RipTag mouse. Relative values to the normal islets are shown. The experiments were repeated with three different mice and representative results are shown (mean ± SD). (**d**) Viability assay the cells in the CTOSs cultured under normoxic (N) or hypoxic (H) conditions for 24 h. Green, calcein-AM; red, PI; blue Hoechst33342. Scale bar, 100 μm.

**Supplementary Figure S6 | VEGF staining of RipTag tumors.**
VEGF staining of the tumors from wt mice (**a**), and HKO mice (**b**).

**Supplementary information**

**Genotype analysis of Hif-1α.** The frozen sections were stained with Hematoxylin and the tumor area was collected by laser micro-dissection (Application Solutions Laser MicroDissection System version 4.1, Leica, Solms, Germany) into a lysis buffer (10% Tween, 1 M Tris-HCl pH 8.0, 0.5 M EDTA, 500 μg/mL Proteinase K). The samples were incubated overnight at 55°C, and subjected as templates to polymerase chain reaction using primers as previously described[2]. Mixed DNA from *Hif-1a*$^{fl/fl}$ and *RipCre/ Hif-1a*$^{fl/fl}$ mice islets were used as a reference.

**Cell culture.** The cell lines from the tumors were established as previously described [3]. The cell lines were maintained in DMEM containing 10% fetal bovine serum (FBS), penicillin G (100 U/mL), and streptomycin (100 μg/mL). The cells were transfected with pMXpuro/CreERT2 as previously described [4], and puromycin-resistant clones were selected in the presence of 3.0 μg/mL puromycin. To delete the Hif-1α gene in the pMXpuro/CreERT2, *Hif-1a*$^{fl/fl}$ cell line, the cells were treated with 100 nM 4-hydroxytamoxifen (H6278, Sigma-Aldrich, St. Louis, MO) and cultured for 24 h.

**Plasmid construction.** DNA encoding CreERT2 [5], was excised from pBLC/CreERT2,

which was derived from pCre-ERT2 (kindly gifted from Dr. Pierre Chambon), at the *EcoRI* site. Two fragments of CreERT2 were subcloned into the *EcoRI* site of the retrovirus vector pMXpuro to generate pMXpuro/CreERT2.

**Islet and tumor isolation.** Isolation of pancreas islets or tumors was performed as previously described with some modification[6]. Briefly, the common bile duct was cannulated, and the pancreas was infused with 2 mg/mL collagenase IV (4186, Worthington, Lakewood, NJ) in HBSS. Pancreases were collected, and protease digestion was continued at 37°C for 17 min. After mechanical dissociation, islets or tumors were visualized and collected with a micropipet under a stereomicroscope (MZFLIII, Leica, Solms, Germany), if necessary. The tumor volume was calculated according to the formula: $0.52 \times (\text{short span})^2 \times \text{long span}$.

**Evaluation of microscopic size of the tumors.** H&E-stained sections of the pancreas were analyzed. The lesions were classified into three groups based on their longest diameter: <200 μm, 200-500 μm, 500-1000 μm. The size of the lesions was represented by the maximum size of the same tumor in the serial sections. Mean ± SD of each genotype mouse is shown. $*P < 0.05$.

**Immunohistochemistry.** The frozen sections were fixed in acetone:methanol (1:1) solution, and blocked with 5% goat serum. For BrdU staining, the sections were treated with HCl before blocking. For NCAM staining, mouse IgG blocking reagent (MKB-2213, VECTOR, Burlingame, CA) was used. Primary antibodies were anti-mouse E-cadherin (M108 1:500 TaKaRa BIO Inc.), anti-N-cadherin (ab18203, 1:500, abcam Tokyo, Japan), anti-NCAM (AG1-s, 1:10, DSHB, Iowa City, IA) , anti-BrdU (555627, 1:50, BD Pharmingen), anti-Insulin (A5064, 1:100,Dako, Carpinteria, CA), anti-HIF (NB100-479,1:500, NOVUS BIOLOGICALS, Littleton, CO), and anti-VEGF (70R-VR001, Fitzgerald Industries International. Inc.). For the whole-mount immunohistochemistry, antibody against E-cadherin (610181, 1:50, BD Pharmingen) was used. The secondary antibodies were biotinylated goat anti-guinea pig IgG, Alexa Fluor 594 goat anti-rat IgG, Alexa Flour 594 goat-anti mouse IgG, Alexa Fluor 594 goat

anti-rabbit IgG, Alexa Fluor 488 goat anti-rabbit IgG, and Alexa Fluor 488 goat anti-mouse IgG. The VECTASTAIN ABC Elite kit (PK-6100, Vector Laboratories) and VECTOR NovaRED SUBSTRATE KIT (SK-4800, Vector Laboratories) were used to detect signal. TUNEL staining was used to identify dead cells using ApopTag Red in Situ Apoptosis Detection Kit (S7165, CHEMICON, Temecula, CA). Hypoxic regions were detected by Hypoxyprobe Plus kit (HP2100, Natural Pharmacia International Inc.). The sections were counterstained with Hoechst 33342 or Hematoxylin and mounted with FluorSave reagent (345789, Calbiochem, Darmstadt, Germany) or EUKITT (O.Kindler, Freiburg, Germany). Whole-mount immunohistochemistry was performed as previously described[7]. After staining, the images were captured by CDD camera (DP50, OLYMPUS, Tokyo, Japan) under a microscope (BX50, OLYMPUS). To evaluate the E-cadherin staining pattern, adjacent exocrine tissue within the same section was used as an internal control. The tumors were classified as "mixed" in which fields of negative or remarkably weak E-cadherin staining were observed. At least three mice from each genotype were analyzed. Quantification of the CD31 staining was performed as previously described[8].

**CTOS viability assay.** For CTOSs, Calcein-AM (1/1000, C3099, Invitrogen, Eugene, Oregon), Propidium Iodide, PI (1/1000, P3566, Invitrogen), and Hoechst33342 (1/1000, H-3570, Invitrogen) were added to the culture medium, and incubated for 20 min at 37°C. Then, the images were captured by CDD camera (CoolSNAP, Photometrics, Tucson, AZ) under the microscope (IX70, OLYMPUS).

**PCR primers for RT-PCR.**

Hif-1α: 5′-CTCCCTTTTTCAAGCAGCAG-3′, 5′-GCATGCTAAATCGGAGGGTA-3′;
Igf2: 5′-GTCGATGTTGGTGCTTCTCA-3′, 5′- AAGCAGCACTCTTCCACGAT-3′;
Gult2: 5′-TTGCTGGCCTCAGCTTTATT-3′, 5′-TCAGTCGATGCCTCTTCCTT-3′;
Glut1: 5′-CTTTGTGTCTGCCGTGCTTA-3′, 5′-GCTGTGCTTATGGGCTTCTC-3′;
Ldha: 5′- AGGCTCCCCAGAACAAGATT-3′, 5′-TCTCGCCCTTGAGTTTGTCT-3′;
Pdk1: 5′-GGCGGCTTTGTGATTTGTAT-3′, 5′-ACCTGAATCGGGGGATAAAC-3′;
E-cadherin: 5′-CAAGGACAGCCTTCTTTTCG -3′, 5′-TGGACTTCAGCGTCACTTTG-3′;

N-cadherin: 5′-CTGGGACGTATGTGATGACG-3′, 5′-GGATTGCCTTCCATGTCTGT-3′;
Ncam: 5′-GATCAGGGGCATCAAGAAAA-3′, 5′-CTATGGGTTCCCCATCCTTT-3′;
Twist: 5′-ACGAGCTGGACTCCAAGATG-3′, 5′-TCCTTCTCTGGAAACAATGACA-3′;
Vimentin: 5′-GAGATCGCCACCTACAGGAA-3′, 5′-GGTCATCGTGATGCTGAGAA-3′;
Tbp (TATA box binding protein):
5′-ACCCTTCACCAATGACTCCTATG-3′, 5′-ATGATGACTGCAGCAAATCGC-3′

**The number of the mice, lesions, or areas, and p-values.**

Figure 1c, Wt: RIP1-Tag2/wt mice ($n$ = 6 mice, 44 tumors); VKO: RIP1-Tag2/VKO mice ($n$ = 7 mice, 28 tumors); RIP1-Tag2: RipTag/DKO mice ($n$ = 3 mice, 8 tumors).

Figure 1d, Wt mice: ($n$ = 9 mice, 315 lesions); VKO mice ($n$ = 10 mice, 355 lesions); DKO mice ($n$ = 10 mice, 506 lesions).
p= 0.0091 (Wt vs. DKO)
p=0.0257 (VKO vs. DKO)

Figure 2b, Wt mice ($n$ = 25 areas from 4 tumors of 3 mice,); VKO mice ($n$ =64 areas from 5 tumors of 4 mice,); DKO mice ($n$ = 75 areas from 7 tumors of 5 mice).
p=0.0026 (Wt vs. VKO)
p<0.0001 (VKO vs. DKO)

Figure 2c, Inside：VKO mice ($n$ =19 areas from 4 tumors of 3 mice), DKO mice ($n$ =20 areas from 4 tumors of 3 mice). Proximal: VKO mice ($n$ = 20 areas from 4 tumors of 3 mice), DKO mice ($n$ = 20 areas from 4 tumors of 3 mice). Distal: Wt mice ($n$ = 25 areas from 4 tumors of 3 mice), VKO mice ($n$ = 25 areas from 5 tumors of 4 mice), DKO mice ($n$ = 25 areas from 5 tumors of 3 mice).
p=0.0002 (VKO vs. DKO, inside)
p=0.0067 (VKO vs. DKO, proximal)
p=0.0346 (VKO vs. DKO, distal)
p=0.0090 (inside vs. proximal, VKO)
p=0.0003 (inside vs. distal, VKO)

Figure 2e, Wt mice ($n$ = 30 areas from 4 tumors of 3 mice); VKO mice ($n$ = 63 areas from 5 tumors of 4 mice ); DKO mice ($n$ = 75 areas from 7 tumors of 5 mice).
p=0.0171 (Wt vs. DKO)
p=0.0055 (VKO vs. DKO)

Figure 2f, Inside: VKO mice ($n$ = 18 areas from 4 tumors of 4 mice), DKO mice ($n$ = 20 areas from 4 tumors of 4 mice). Proximal: VKO mice ($n$ = 20 areas of 4 tumors of 4 mice), DKO mice ($n$ = 20 areas from 4 tumors of 4 mice). Distal: Wt mice ($n$ = 30 areas from 6 tumors of 3 mice), VKO mice ($n$ = 25 areas from 5 tumors of 5 mice), DKO mice ($n$ = 35 areas from 7 tumors of 5 mice).
p=0.0008 (Wt vs. DKO, distal)
p=0.0066 (VKO vs. DKO, distal)

Figure 3b, Wt mice ($n$ = 9 mice, 315 lesions); VKO mice ($n$ = 10 mice, 355 lesions); DKO mice ($n$ = 10 mice, 506 lesions).
p=0.0353 (VKO vs. DKO, IC1)
p=0.0031 (Wt vs. VKO, IC2)
p=0.0078 (VKO vs. DKO, IC2)

Figure 3e, Wt mice ($n$ = 6 mice, 14 invasive tumors), VKO mice ($n$ = 5 mice, 48 invasive tumors), DKO mice ($n$ = 5 mice, 21 invasive tumors).
p=0.0034 (Wt vs. VKO)
p=0. 0147 (VKO vs. DKO)

Supplementary References

1 Postic, C. *et al.* Dual roles for glucokinase in glucose homeostasis as determined by liver and pancreatic beta cell-specific gene knock-outs using Cre recombinase. *The Journal of biological chemistry* **274**, 305-315 (1999).

2 Tomita, S. *et al.* Defective brain development in mice lacking the Hif-1alpha gene in neural cells. *Molecular and cellular biology* **23**, 6739-6749 (2003).

3 Efrat, S. *et al.* Beta-cell lines derived from transgenic mice expressing a hybrid insulin gene-oncogene. *Proceedings of the National Academy of Sciences of the United States of America* **85**, 9037-9041 (1988).

4 Inoue, M. *et al.* Targeting hypoxic cancer cells with a protein prodrug is effective in experimental malignant ascites. *International journal of oncology* **25**, 713-720 (2004).

5 Feil, R., Wagner, J., Metzger, D. & Chambon, P. Regulation of Cre recombinase activity by mutated estrogen receptor ligand-binding domains. *Biochemical and biophysical research communications* **237**, 752-757 (1997).

6 Parangi, S., Dietrich, W., Christofori, G., Lander, E. S. & Hanahan, D. Tumor suppressor loci on mouse chromosomes 9 and 16 are lost at distinct stages of tumorigenesis in a transgenic model of islet cell carcinoma. *Cancer research* **55**, 6071-6076 (1995).

7 Weiswald, L. B. *et al.* In situ protein expression in tumour spheres: development of an immunostaining protocol for confocal microscopy. *BMC cancer* **10**, 106 (2010).

8 Paez-Ribes, M. *et al.* Antiangiogenic therapy elicits malignant progression of tumors to increased local invasion and distant metastasis. *Cancer cell* **15**, 220-231 (2009).